Nucleon-nucleon cross sections in nuclear matter

H.-J. Schulze,* A. Schnell, and G. Röpke
MPG-AG ''Theoretische Vielteilchenphysik,'' Universität Rostock, D-18051 Rostock, Germany

U. Lombardo
Dipartimento di Fisica, Università di Catania, Corso Italia 57, I-95129 Catania, Italy
(Received 20 December 1996)

We provide a microscopic calculation of neutron-proton and neutron-neutron cross sections in symmetric nuclear matter at various densities, using the Brueckner-Hartree-Fock approximation scheme with the Paris potential. We investigate separately the medium effects on the effective mass and on the scattering amplitude. We determine average cross sections suitable for application in the dynamical simulation of heavy ion collisions, including a parametrization of their energy and density dependence. [S0556-2813(97)01605-1]

PACS number(s): 25.70.−z, 13.75.Cs, 21.65.+f, 24.10.Cn

I. INTRODUCTION

The knowledge of the in-medium modification of nucleon-nucleon cross sections is of great interest for the numerical simulation of heavy ion collisions [1–7]. At intermediate energies of the order of 100 MeV/nucleon a transition from a mean field regime to a hydrodynamic collective motion occurs. It is signaled by the vanishing of the sideward collective flow at the balance energy, due to the compensation between the low-energy attractive effect of the mean field and the repulsive action of nucleon-nucleon collisions dominant at higher energies. We expect this collective variable to be quite sensitive to the high-density behavior of the in-medium nucleon-nucleon cross sections. In fact, some theoretical predictions using free cross sections largely underestimate the experimental values of the balance energy calculated for a wide range of the combined mass of the two colliding nuclei, whereas a reduction of cross sections of typically 20% leads to a better, but still not satisfactory agreement [1,2]. A further observable sensitive to the cross sections is the radial flow energy which is due to the conversion of thermal and compressional energy to collective energy mediated by the NN scatterings in the latest stages of a central collision. At low enough density when the scattering probability vanishes, freeze-out occurs and the energy conversion stops. The magnitude of the freeze-out time determines the content of radial flow energy. If a suppression of the cross sections is predicted at low density, freeze-out occurs earlier and a suppression of the radial flow energy has to be expected, too. Recent calculations confirm, in fact, this prediction [1].

Numerous theoretical studies have been carried out in order to gain insight in the effect of a dense nuclear medium on the scattering amplitudes and cross sections: All the calculations performed so far rely on the condition of local thermal equilibrium, i.e., they assume that during the evolution of the collision the momentum distribution of nucleons in a given coordinate-space cell is well approximated by either one [8–12] or two [7,13] Fermi spheres of certain density and temperature. For this configuration the Brueckner [7,8,12] or Dirac-Brueckner [9,11,13] G matrix (or thermodynamic T matrix [10]) is computed by summing up multiple particle-particle (and hole-hole) interactions. In this paper we will remain within this framework and discuss the case of infinite nuclear matter at zero temperature with the Brueckner G matrix. The scattering amplitudes obtained in this way thus incorporate the effects of nuclear mean field and Pauli blocking in the intermediate propagation of nucleon pairs. The second ingredient necessary to calculate cross sections is the density of states in the medium that is proportional to the (momentum dependent) effective mass of the nucleons. It is one purpose of this paper to disentangle these two contributions, i.e., the modification of the G-matrix elements, and the change of the density of states in the medium. It turns out that the latter effect strongly overwhelms the first one which by itself would lead to an increase of cross sections with density.

Unfortunately, for the sake of practical application, the in-medium cross section is a function of too many variables: Besides the dependence on scattering angle ϑ and relative momentum k, as in the free scattering case, there is now a dependence on total momentum P and total energy W of the nucleon-nucleon pair, as well as on density ρ and temperature T of the medium (even more parameters for the case of two colliding Fermi spheres, which will be discussed later). Moreover, in certain regions of this multiparametric space, the cross section might be strongly varying, as, for example, in the case $P \approx 0$, $k \approx k_F$, where one observes at low temperatures and densities a strong enhancement of the cross section due to the onset of pairing [10,12].

In order to facilitate a practical application in numerical simulations, we will provide in this work simple (quadratic) parametrizations of the density dependence of effective, average total neutron-neutron and neutron-proton cross sections that depend just on one momentum variable. The averaging procedure we carry out is in line with the occurence of the cross section in the collisional integral of the BUU equation, and relates the average cross section to the imaginary part of the in-medium nucleon self-energy. More precisely, the collision partner of a nucleon with given momentum is averaged over the Fermi sphere, taking into account the Pauli blocking of the final state. The dependence on several vari-

*Present address: Sezione INFN, Università di Catania, Corso Italia 57, I-95129 Catania, Italy.

ables is removed in this way, and we extract a correction factor describing the momentum dependent modification of cross sections in the medium, in the spirit of Ref. [8]. It is hoped that this factor retains the most prominent dynamical effects and can be used realistically in the numerical simulation of heavy ion collisions. It should be noted, however, that for this purpose the relevant quantity is not the cross section, but the reaction rate, proportional to the product of relative velocity and cross section. We present results for the modification of this observable as well.

Obviously, for reliable and realistic predictions, the use of a good nucleon-nucleon interaction is mandatory. The results reported in this paper are obtained with the Paris potential [14] which is known to be in very good agreement with free scattering phase shifts up to energies $E_{\rm lab}\approx 400$ MeV, where inelastic processes start to play a role, anyway. Partial waves up to ${}^3I_6$ are summed for the calculation of cross sections. We have also carried out independent calculations using the Argonne V_{14} potential [15], and the results do not deviate substantially from those with the Paris potential, whereas a separable version of the Paris potential [16] turned out to be insufficient for $E_{\rm lab}\gtrsim 150$ MeV.

II. FORMALISM

We start with an overview of the calculation of cross sections in Brueckner theory [17,18]. The construction of the in-medium G matrix is based on the solution of the Bethe-Goldstone equation for the correlated wave function u in the various nucleon-nucleon channels characterized by discrete quantum numbers T,S,J,L,L':

$$u^{TSJ}_{LL'}(W,P,k,r)=j_L(kr)\,\delta_{LL'} +4\pi\int_0^\infty dr' r'^2 D_{L'}(W,P,r,r') \times\sum_{L''} V^{TSJ}_{L'L''}(r')\; u^{TSJ}_{LL''}(W,P,k,r') \quad (1)$$

with the intermediate propagator

$$D_{L'}(W,P,r,r') =-\frac{1}{2\pi^2}\int_0^\infty dk''\; k''^2\,\frac{j_{L'}(k''r)j_{L'}(k''r')Q(P,k'')}{W-E(P,k'')+i\epsilon}\;, \quad (2)$$

and

$$W=e(p_1)+e(p_2),\quad e(p_i)=\frac{p_i^2}{2m}+\mathrm{Re}\;U(p_i)\;, \quad (3)$$

$$Q(P,k'')=\max\left[0,\min\left[\frac{P^2/4+k''^2-k_F^2}{Pk''},1\right]\right]\;, \quad (4)$$

$$E(P,k'')=e(p_+)+e(p_-),\;\; p_\pm^2=\frac{P^2}{4}+k''^2\pm\frac{Q(P,k'')}{\sqrt{3}}Pk''\;. \quad (5)$$

Here W is the starting energy of the initial nucleon pair with total momentum $P=|\mathbf{p}_1+\mathbf{p}_2|$ and relative momentum $k=|\mathbf{p}_2-\mathbf{p}_1|/2$, and $Q(P,k'')$, $E(P,k'')$ are the Pauli operator and energy of the intermediate nucleon pair with relative momentum k'', respectively. The single-particle potential U is determined self-consistently along with the G matrix.

The Pauli operator and two-nucleon energy are angle averaged in order to allow a partial wave expansion of the G matrix in the form

$$\langle TS\nu'\mathbf{k}'|G(W,P)|\mathbf{k}\nu ST\rangle=\sqrt{4\pi}\sum_{J,L,L'}\sqrt{2L+1} \times\langle L'S\mu\nu'|J\nu\rangle\langle LS0\nu|J\nu\rangle \times G^{TSJ}_{LL'}(W,P,k',k)\;Y_{L'\mu}(\vartheta,\varphi) \quad (6)$$

($\nu,\nu',\mu=\nu-\nu'$ indicating spin orientation). The solutions of the Bethe-Goldstone equation determine the G-matrix elements

$$G^{TSJ}_{LL'}(W,P,k',k)=4\pi\int_0^\infty dr\; r^2\; j_L(k'r) \times\sum_{L''} V^{TSJ}_{LL''}(r)\; u^{TSJ}_{L''L'}(W,P,k,r)\;, \quad (7)$$

and the single-particle potentials are then given by the diagonal elements

$$U(p_1)=\sum_{T,S,J,L}\frac{(2T+1)(2J+1)}{(2t_1+1)(2s_1+1)}\,\frac{2}{(2\pi)^3} \times\int d^3p_2 f(p_2)\; G^{TSJ}_{LL}(W,P,k,k) \quad (8)$$

with the Fermi distribution $f(p)=\theta(k_F-p)$, which, combined with the previous equations, constitutes the self-consistency problem.

The (dimensionless) in-medium nucleon-nucleon on-shell scattering amplitudes a are related to the G-matrix elements by

$$a^{TSJ}_{LL'}(W,P,k)=-\frac{kM^*(P,k)}{4\pi}G^{TSJ}_{LL'}(W,P,k,k), \quad (9)$$

and consequently depend on energy W and total momentum P of the nucleon pair besides on its relative momentum k and quantum numbers T,S,J,L,L'. The effective mass of the two-nucleon system is given by

$$M^*(P,k)=\left[\frac{\partial E(P,k)}{\partial k^2}\right]^{-1}\;. \quad (10)$$

For a parabolic single-particle potential (constant effective mass), and in general for $P=0$, the two-nucleon effective mass coincides with the nucleon effective mass: $M^*(0,k)=m^*(k)=[2\partial e(k)/\partial k^2]^{-1}$. For the nontrivial case of mixing by the tensor interaction, the standard parametrization [19] of the free amplitudes ($\rho=0$) in terms of phase shifts δ and mixing angle ϵ is as follows ($L'=L+2$):

$$\begin{pmatrix} a_{LL} & a_{LL'} \\ a_{L'L} & a_{L'L'} \end{pmatrix} = \begin{pmatrix} \frac{1}{2i}[\cos(2\epsilon)\exp(2i\delta_L)-1] & -\frac{1}{2}\sin(2\epsilon)\exp\ i(\delta_L+\delta_{L'}) \\ -\frac{1}{2}\sin(2\epsilon)\exp\ i(\delta_L+\delta_{L'}) & \frac{1}{2i}[\cos(2\epsilon)\exp(2i\delta_{L'})-1] \end{pmatrix} . \tag{11}$$

For the uncoupled partial waves we have $\epsilon=0$ and the usual parametrization of amplitudes a in terms of phase shifts δ.

The unpolarized elastic differential and total cross sections in the isospin $T=0,1$ channels are given in terms of G-matrix elements and scattering amplitudes by [20]

$$\frac{d\sigma_T}{d\Omega}(W,P,k,\vartheta)=\frac{1}{(2s_1+1)(2s_2+1)}\sum_{S,\nu,\nu'}\left|-\frac{M^*(P,k)}{4\pi}\langle TS\nu'\mathbf{k}'|G(W,P)|\mathbf{k}\nu ST\rangle_A\right|^2 , \tag{12a}$$

$$\sigma_T(W,P,k)=\frac{4\pi}{k^2}\frac{2}{(2s_1+1)(2s_2+1)}\sum_{J,S,L,L'}(2J+1)|a_{LL'}^{TSJ}(W,P,k)|^2 , \tag{12b}$$

from which the neutron-neutron, neutron-proton, and nucleon-nucleon cross sections can be obtained:

$$\sigma_{nn}=\sigma_1 , \tag{13a}$$

$$\sigma_{np}=\tfrac{1}{2}(\sigma_0+\sigma_1) , \tag{13b}$$

$$\sigma_{NN}=\tfrac{1}{2}(\sigma_{nn}+\sigma_{np})=\tfrac{1}{4}(\sigma_0+3\sigma_1) . \tag{13c}$$

The resulting cross sections exhibit the interesting feature of a strong enhancement in the case of zero total momentum when the interacting nucleons approach the Fermi surface [21], which reflects the possibility of the two nucleons being able to form a Cooper pair. This can clearly be seen when considering the propagator Eq. (2) in this case:

$$D_L(W,0,r,r')=-\frac{1}{2\pi^2}\int_{k_F}^{\infty}dk\ k^2\ \frac{j_L(kr)j_L(kr')}{W-2e(k)+i\epsilon} , \tag{14}$$

which is singular for $W\to 2e_F$ due to the use of continuous single-particle energies in the denominator. In fact at this point the BHF scheme breaks down and should be supplemented by a consistent treatment of pairing gaps [22,23]. This enhancement makes an empirical parametrization of the cross sections rather difficult. However, the effect is only important for the total momentum close to zero, and a sharp single Fermi surface (zero temperature, infinite nuclear matter). At the same time, at this point there is a strong suppression of the physical scattering process due to the Pauli blocking of the final state that is not included in the definition of the cross sections Eq. (12). For all these reasons we seek for some method to dispose of this effect by averaging the cross sections in a meaningful way. This averaging will also remove their dependence on W, P (and ϑ), that prevents a simple understanding of the various effects of the nuclear medium where the NN collisions occur, and, more importantly, prevents a simple application in dynamical simulations of heavy ion collisions. Therefore average cross sections have been proposed [8,9,13] that are more suitable for clarifying the separate effects of effective mass, single-particle spectrum and Pauli blocking. We remind the reader that the main physical assumption underlying the use of such effective cross sections [but also the cross sections as such, Eq. (12)] is the local thermal equilibrium which has to be expected in heavy ion collisions for beam energies not too far from the Fermi energy. Otherwise, the G matrix should be recalculated for each time step during the dynamical evolution of the distribution function $f(\mathbf{p},\mathbf{r},t)$ in each space point $\mathbf{r}$. This task is for the time being prohibitive, even if we stick to a local density approximation.

For the purpose of averaging we consider the following collisional integrals that provide a weighting of the in-medium cross sections with the final state Pauli operator and the relative velocity of the reacting nucleons (we suppress the isospin index now):

$$I_{\rm loss}(p_1)=\int d^3p_2d^3p_3d^3p_4\ f(p_2)\overline{f}(p_3)\overline{f}(p_4)\delta^3(\mathbf{p}_1+\mathbf{p}_2-\mathbf{p}_3-\mathbf{p}_4)\delta(e_1+e_2-e_3-e_4)\ \overline{\sum_{\rm spin}}|\langle 34|G|12\rangle_A|^2 \tag{15}$$

$$\approx 16\pi^2\int d^3p_2 f(p_2)\ Q_{pp}(P,k)\frac{k}{M^*(P,k)}\sigma^*(W,P,k) , \tag{16}$$

$$I_{\rm gain}(p_1)=\int d^3p_2d^3p_3d^3p_4\ \overline{f}(p_2)f(p_3)f(p_4)\delta^3(\mathbf{p}_1+\mathbf{p}_2-\mathbf{p}_3-\mathbf{p}_4)\delta(e_1+e_2-e_3-e_4)\ \overline{\sum_{\rm spin}}|\langle 34|G|12\rangle_A|^2 \tag{17}$$

$$\approx 16\pi^2\int d^3p_2\overline{f}(p_2)\ Q_{hh}(P,k)\frac{k}{M^*(P,k)}\sigma^*(W,P,k) , \tag{18}$$

with the Fermi function $f(p)$ and $\overline{f(p)} := 1 - f(p)$. The appearance of the effective mass of the two-nucleon system, Eq. (10), is due to the energy-conserving δ function in Eqs. (15) and (17). The in-medium cross section $\sigma^*(W,P,k)$ was defined in Eq. (12b) (the star denoting the difference to the free cross section, obtained with the free nucleon mass, $M^* \to m$, and the free T matrix, $G \to T$). In order to arrive at Eqs. (16) and (18), it was, in line with the G-matrix calculation, necessary to carry out an angle average for the Pauli operator $f_3 f_4 \to Q_{pp}(P,k)$, $f_3 f_4 \to Q_{hh}(P,k)$, and energy $(e_3 + e_4) \to E(P,k)$ of the final state. The Pauli operators for a particle-particle or hole-hole pair are explicitly given by

$$Q_{pp}(P,k) = \max[0, \min[+z(P,k), 1]] \ , \tag{19a}$$

$$Q_{hh}(P,k) = \max[0, \min[-z(P,k), 1]] \ , \tag{19b}$$

$$z(P,k) = \frac{P^2/4 + k^2 - k_F^2}{Pk} \ .$$

For the zero-temperature case that we are considering here, the loss integral is nonzero only for $p_1 > k_F$, and the gain integral only for $p_1 < k_F$. In fact, the isospin-averaged integral Eq. (15) is by a dispersion relation closely related to the imaginary part of the single-particle potential [8,13,18]:

$$I^{NN}_{\rm loss}(p_1) = -(2\pi)^5 \ {\rm Im} \ U(p_1) \ . \tag{20}$$

In the same manner the gain contribution to the collisional integral is related to the imaginary part of the rearrangement contribution U_2 to the mean field [24]:

$$I^{NN}_{\rm gain}(p_1) = -(2\pi)^5 \ {\rm Im} \ U_2(p_1) \ . \tag{21}$$

These relations provide an independent check of the numerical procedure.

Guided by the expression Eq. (16) we define the following average cross sections:

$$\langle \sigma \rangle_1(p_1) := \frac{\int d^3p_2 f(p_2) \ Q(P,k) \ [k/M^*(P,k)] \ \sigma^*(W,P,k)}{\int d^3p_2 f(p_2) \ [k/M^*(P,k)]} \ , \tag{22a}$$

$$\langle \sigma \rangle_2(p_1) := \frac{\int d^3p_2 f(p_2) \ Q(P,k) \ [k/M^*(P,k)] \ \sigma(W,P,k)}{\int d^3p_2 f(p_2) \ [k/M^*(P,k)]} \ , \tag{22b}$$

$$\langle \sigma \rangle_3(p_1) := \frac{\int d^3p_2 f(p_2) \ Q(P,k) \ [k/M^*(P,k)] \ \sigma(k)}{\int d^3p_2 f(p_2) \ [k/M^*(P,k)]} \ . \tag{22c}$$

These definitions are valid for $p_1 > k_F$; in the case $p_1 < k_F$ we use the corresponding gain integrals, i.e., we substitute $f(p_2) \to \overline{f}(p_2)$ and $Q(P,k) \to Q_{hh}(P,k)$. Also, in this case an upper limit to the normalization integral in the denominator has to be provided. We use here $p_{2\max} = \sqrt{2} k_F$, which is the maximum value the momentum p_2 can assume in the numerator.

The first definition (22a) is most closely related to the collisional integral by weighting the in-medium cross section with the relative velocity of the reacting nucleons. Definition (22b) uses an in-medium cross section $\sigma(W,P,k)$ evaluated with the free nucleon mass instead of the effective mass, i.e., $M^*(P,k)$ is replaced by m in Eqs. (9) and (12a) (but *not* in the calculation of the G-matrix elements themselves). This allows one to extract the modification of the squared G-matrix elements alone, disregarding the change of the density of states in the medium. Finally, as a reference value, definition (22c) uses the free cross section $\sigma(k)$, obtained with the free nucleon mass and free T matrix.

Our main interest, however, lies not in these effective cross sections themselves, but in the ratios $C_i(p_1) := \langle \sigma \rangle_i(p_1) / \langle \sigma \rangle_3(p_1)$, $i = 1,2$, which signal the importance of in-medium corrections relative to the free cross section for the scattering process of a nucleon with momentum p_1. In particular, if $C_1(p_1)\sigma(k)$ would be used in the collisional integral, one would obtain the same result as evaluated with the full in-medium cross section $\sigma^*(W,P,k)$. The function C_1 is therefore of great practical use as a scaling factor for the free cross section in the numerical simulation.

For the actual calculation of Eqs. (22), particular attention has to be paid to the case $p_1 \to k_F$, because then the momenta p_2 of the Pauli-allowed reaction partners are located within a thin shell at the Fermi surface, and the integrand is a strongly varying function of the angle between $\mathbf{p}_1$ and $\mathbf{p}_2$. This has observable consequences that will be discussed later.

III. RESULTS

We come now to the presentation of our results: We begin in Fig. 1 with a plot of self-consistent single-particle potentials (real and imaginary part) and effective masses. A characteristic feature here is the well-known local enhancement

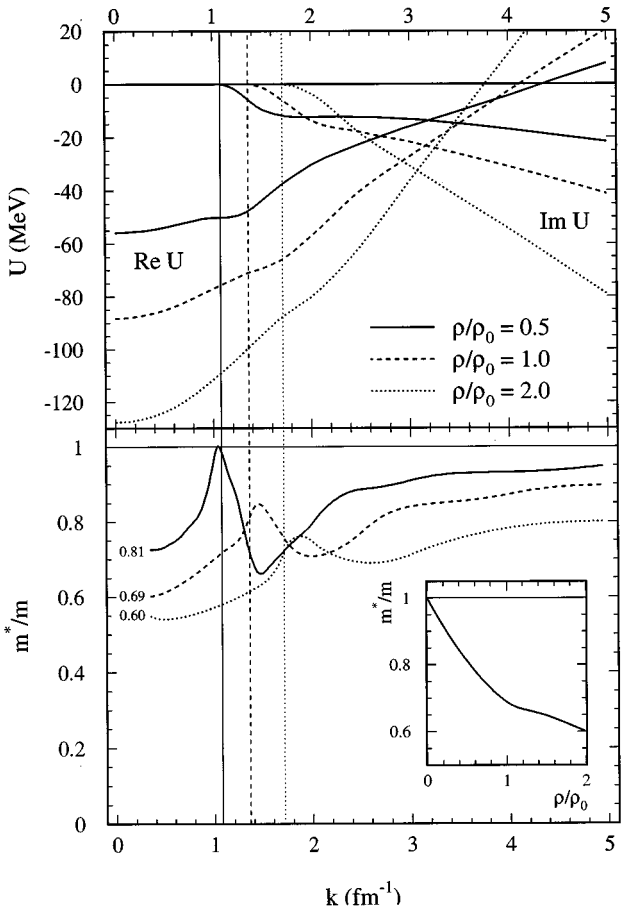

FIG. 1. BHF single-particle potentials (upper panel) and effective masses (lower panel) at three densities $\rho/\rho_0 = 0.5,1,2$. The vertical lines denote the positions of the corresponding Fermi momenta $k_F = 1.08, 1.36, 1.71$ fm^{-1}. The inset in the lower panel shows the variation of the *global* effective mass (in the range $k = 0, \ldots, k_F$) with density. The values according to this plot are indicated to the left of the curves in the lower panel.

of the effective mass near the Fermi surface [18]. This enhancement becomes more prominent with decreasing density, and in fact prohibits a self-consistent solution of the BHF scheme below $k_F \approx 0.8$ fm^{-1} ($\rho/\rho_0 \approx 0.2$). A fully self-consistent treatment of single-particle energies and the appearance of pairing gaps and bound states at low densitites is at the moment not available [22,23]. It can be concluded from this figure that the use of a constant effective mass [8–10] is not appropriate for the determination of energy dependent in-medium cross sections.

These single-particle potentials and effective masses are used in the evaluation of (average) cross sections according to Eqs. (12) and (22). A first check of the numerical scheme is the calculation of free scattering phase shifts and cross sections. These turn out to be in excellent agreement with the results for the phase shifts given in the original reference [14], as well as with experimental data on total cross sections [25]. The free neutron-proton and neutron-neutron cross sections are displayed in Fig. 2, where we also show for the sake of comparison the results obtained with the Argonne V_{14} potential [15], and with a separable parametrization of the Paris potential [16]. The agreement with the Argonne results (which are based on partial waves up to $J = 5$ as the Paris calculation) is very good, the deviation at large scattering energies in the neutron-neutron channel being mainly due to differences in the $^3PF_2$ phase shifts, which do not completely agree in both potentials. The separable parametrization of the Paris potential can only be used reliably up to $E \approx 150$ MeV. Apart from the missing higher partial waves ($J \leqslant 2$), there are substantial deviations from the experimental results in particular in the P partial waves at higher energies.

In the same Fig. 2, we show the in-medium cross sections $\sigma^*(W,P,k)$ and $\sigma(W,P,k)$ at nuclear matter density as functions of the laboratory energy $E = (2k)^2/2m$ for two different configurations in momentum space: $P = 0$ [the two nucleons having opposite momenta, $p_1 = p_2 = k$, $W = 2e(k)$]; and $P = 2k$ [one nucleon at rest, $p_1 = 0$, the other with momentum $p_2 = P = 2k$, $W = e(0) + e(2k)$]. In general, besides at very low energies, the in-medium cross sections $\sigma(W,P,k)$ neglecting the modification of the density of states are *enhanced* compared to the free ones. This enhancement is however completely overcome by the reduction of the effective mass, so that a sizable suppression results for the physical cross sections $\sigma^*(W,P,k)$. Comparing the two configurations displayed, a prominent feature is the pairing singularity at $k = k_F$ for $P = 0$. Any finite value of the total momentum (and/or deviation from our assumptions of zero temperature and an infinite system) will however reduce this singularity to a mere enhancement of the cross section, as for example in the second configuration displayed. (In fact in this case most of the enhancement is due to the momentum dependence of the effective mass.) Apart from the pairing singularity, we observe large quantitative differences between the two configurations, which demonstrates that in a practical application the rather arbitrary restriction to $P = 0$ [7,11,12] is not justified.

In Fig. 3 we display the average nucleon-nucleon (i.e., isospin averaged) cross sections $\langle\sigma\rangle_1$, $\langle\sigma\rangle_2$, $\langle\sigma\rangle_3$, as well as the ratios $\langle\sigma\rangle_1/\langle\sigma\rangle_3$ and $\langle\sigma\rangle_2/\langle\sigma\rangle_3$ as functions of the momentum p_1 for three different densities. The results shown in this figure are for $p_1 > k_F$ based on the loss integral Eq. (15), and for $p_1 < k_F$ on the gain integral Eq. (17). As noted above, the in-medium cross section $\langle\sigma\rangle_1$ is reduced with respect to the free one, $\langle\sigma\rangle_3$, whereas there is a sizable enhancement when neglecting the change of the density of states, as in $\langle\sigma\rangle_2$. The medium modification of the density of states due to a reduction of the effective nucleon mass obviously completely outweighs the intrinsic enhancement of scattering amplitudes. In particular at low densities, and when the momentum p_1 approaches the Fermi momentum from above, there is a strong competition between the the rise of the microscopic cross sections, Eq. (12b), and the onset of Pauli blocking, leading to a local maximum of the average cross sections. Ultimately, however, the complete Pauli blocking forces the average cross sections to vanish at the Fermi momentum. For sufficiently large momenta (in fact beyond the maximum value $p_1 = 5$ fm^{-1} that we display) all average cross sections approach the free cross section $\sigma(k)$. These curves can be compared with similar results of Ref. [9] in the framework of relativistic Dirac-Brueckner theory with a different potential. We find a qualitative agreement, although in general the in-medium suppression is stronger in that work.

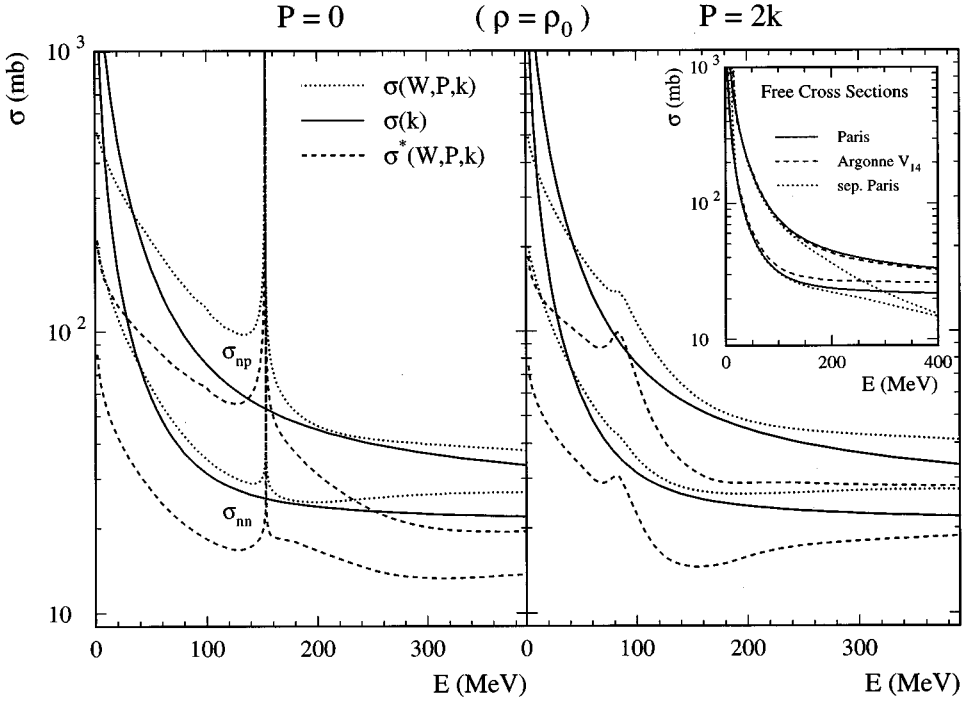

FIG. 2. In-medium total neutron-proton and neutron-neutron cross sections at nuclear matter density for vanishing total momentum, $P=0$ (left), and for the configuration $P=2k$ (right). The dashed curves include the in-medium modification of the density of states; the dotted curves do not. The full curves represent the free cross sections for comparison. The inset compares the free cross sections evaluated with different potentials.

This can be traced back to smaller values of (global) effective nucleon masses that were used.

Coming to the ratios of average cross sections, as displayed in the lower part of Fig. 3, the prominent feature is a pronounced reduction of the ratio $\langle\sigma\rangle_2/\langle\sigma\rangle_3$ on the Fermi surface, i.e., for $p_1 \rightarrow k_F$. (The transition from the loss integral to the gain integral is continuous at this point.) This is due to the strong increase of the free cross section with van-

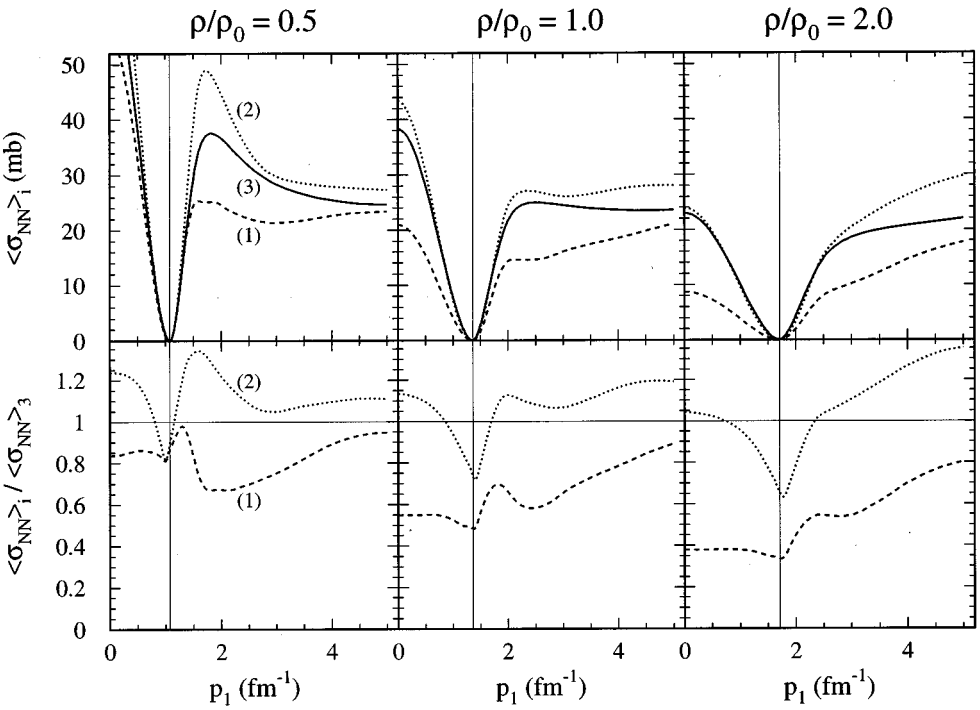

FIG. 3. Top row: Average nucleon-nucleon cross sections at three densities $\rho/\rho_0=0.5,1,2$ as functions of momentum p_1. The numbers in brackets indicate the type i of cross section according to Eq. (22). Bottom row: ratios of average in-medium and free cross sections. The vertical lines denote the positions of the Fermi momentum.

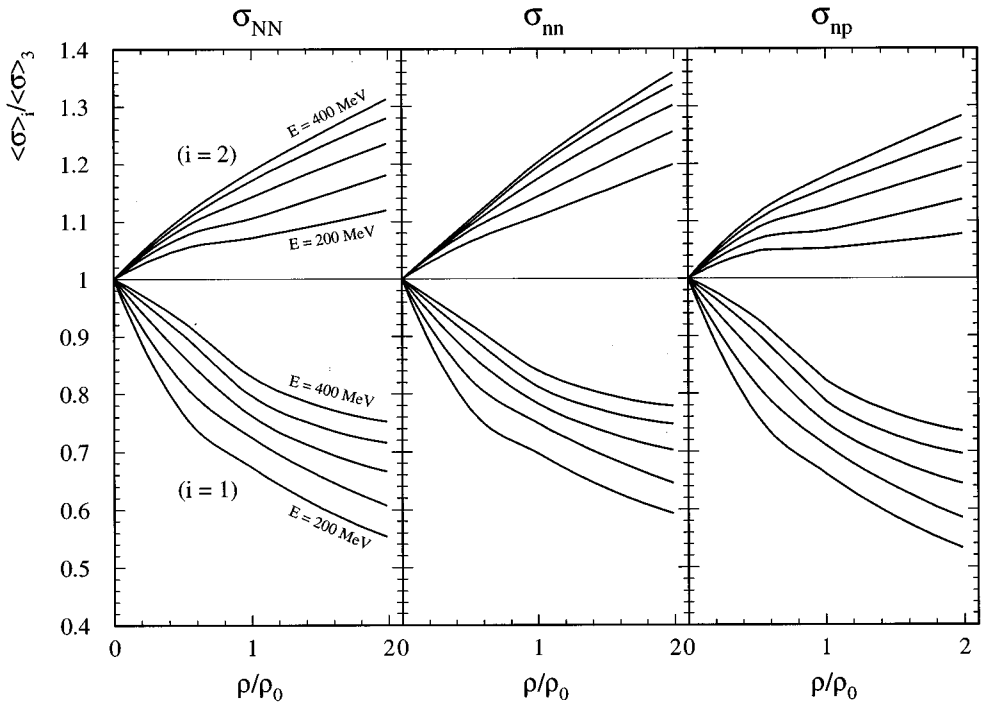

FIG. 4. Ratio of average in-medium and free cross sections, Eq. (22), as a function of density for different energies $E=200,\ldots,400$ MeV in steps of 50 MeV.

ishing relative momentum that is probed in this kinematical situation, as mentioned above. For the ratio $\langle\sigma\rangle_1/\langle\sigma\rangle_3$ this reduction is partly removed due to the local enhancement of the effective mass near the Fermi surface and a smoother curve results. The local maximum of the ratios at low densities and for momenta slightly above the Fermi surface is linked to the increase of the nonaveraged in-medium cross sections for momenta in this range, as seen in Fig. 2. We remark, however, that these variations in the vicinity of the Fermi surface are low-energy features that depend strongly on the temperature of the system [8,10] and on details of the averaging procedure. In this work we will concentrate on the situation at large momenta $p_1 \gtrsim 3$ fm^{-1}, which is more stable against increase of temperature. Comparing our results for $\langle\sigma\rangle_2/\langle\sigma\rangle_3$ with the equivalent ones of Ref. [8], we find quantitative deviations that might be due to the fact that in that reference the free and in-medium collisional integrals were not calculated in the same manner, and, perhaps more important, that a constant effective mass was used.

Our main interest lies in the density dependence of the cross sections, which is displayed in Fig. 4 separately for the nucleon-nucleon, neutron-neutron, and neutron-proton channels. We plot there the ratios $\langle\sigma\rangle_1/\langle\sigma\rangle_3$ and $\langle\sigma\rangle_2/\langle\sigma\rangle_3$ for different average scattering energies $E:=p_1^2/2m$. (The scattering energy is defined as the kinetic energy of one particle in the frame where the second one is at rest.) In the range 200 MeV$<E<$400 MeV we observe a smooth and monotonic behavior of the resulting curves. We find that the dependence on the density of the ratio $\langle\sigma\rangle_2/\langle\sigma\rangle_3$ is to a very good extent linear, whereas the nonlinear dependence of the effective mass on density (see Fig. 1) renders the ratio $\langle\sigma\rangle_1/\langle\sigma\rangle_3$ to be reasonably well described by a quadratic fit of the form

$$\frac{\langle\sigma\rangle_i}{\langle\sigma\rangle_3}(E,\rho)\approx 1+\alpha_i(E)\frac{\rho}{\rho_0}-\beta_i(E)\left(\frac{\rho}{\rho_0}\right)^2 . \qquad (23)$$

The coefficients $\alpha_i(E),\beta_i(E)$ of this fit are shown in Fig. 5, where we finally compare results obtained with the Paris and the Argonne V_{14} potential. It is reassuring to see that both potentials predict nearly identical results outside their originally intended scope of application. We find only small differences between the neutron-neutron and neutron-proton channel, with slighty stronger reduction of the latter in the medium in the case of the Paris potential. The substantial energy dependence of the coefficients α and β reflects the fact that the influence of the medium is more pronounced at low energies where the cross sections are more strongly suppressed. In fact we note that this dependence on energy is to a good approximation linear, which leads ultimately to the following very simple parametrization of the in-medium nucleon-nucleon cross section:

$$\frac{\langle\sigma\rangle_1}{\langle\sigma\rangle_3}(E,\rho)\approx 1-\left[0.63-0.21\frac{E}{E_0}\right]\frac{\rho}{\rho_0}+\left[0.16-0.06\frac{E}{E_0}\right]\left(\frac{\rho}{\rho_0}\right)^2,$$

$$E_0=200\ \text{MeV}\ , \qquad (24)$$

valid in the range $E_0<E<2E_0$ and $0<\rho<2\rho_0$.

It should however be emphasized that below $E\approx 200$ MeV these quadratic fits of the cross section ratios do no longer apply. Rather one observes there a nonmonotonic behavior which reflects the strong variation of the ra-

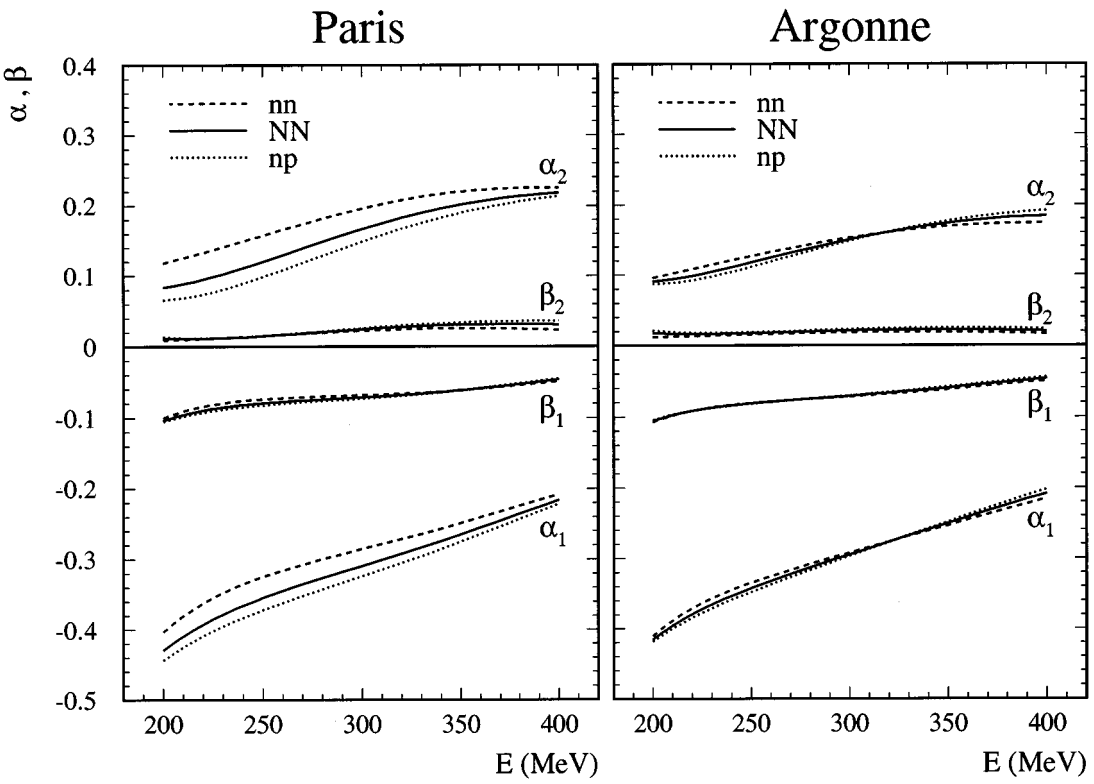

FIG. 5. Coefficients of a parabolic fit of the density dependence of average cross section ratios, Eq. (23), for calculations with the Paris or the Argonne V_{14} potential.

tios displayed in Fig. 3 when approaching the Fermi momentum corresponding to a given density. Fortunately, in this low energy domain the Pauli blocking becomes operative, so that a less accurate treatment is perhaps possible. Very roughly, the suppression of cross sections at nuclear matter density is about 20–30 % with a sizable dependence on the scattering energy, in accordance with previous estimates [9–13]. A suppression of such order of magnitude seems to be necessary to reproduce the experimental power law for the balance energy as a function of the mass of the two combined ions [1,2]. But we guess that the agreement might be improved if one includes a sensitive energy dependence according to our findings.

We finally remark that our results in Fig. 3 also display a strong reduction of the cross sections for collisions bringing nucleons to unoccupied states below the Fermi momentum, due to the small values of the effective mass relevant here. (For example, the suppression is larger than 40% at nuclear matter density.) These processes contribute to the gain part of the collisional integral.

IV. DISCUSSION AND CONCLUSIONS

This paper mainly addresses the microscopic description of heavy ion collisions. In a wide range of the bombarding energy the dynamics of these reactions is driven by the competition between the nuclear mean field and the *NN* scatterings from the early stage up to freeze-out. A collective observable that is very sensitive to this competition is the balance energy since it marks the transition from negative to positive sideward flow. This is the reason why, in dynamical simulations, it is important to make use of an equation of state where the medium effects are consistently incorporated in the mean field as well as in the *NN* cross sections. This consistency can only be provided by a microscopic framework such as the Brueckner theory which is of concern in the calculation of the *NN* cross sections presented and discussed here. The input *NN* interaction in our calculations is the full Paris potential that provides a fine reproduction of the experimental phase shifts for elastic nucleon-nucleon collisions. Due to the dependence of the cross sections on many variables an averaging procedure based on collisional integrals is proposed that, while keeping the main medium effects, yields momentum and density dependent average cross sections quite suitable to use in dynamical simulations. These average cross sections are substantially suppressed with respect to the free cross sections due to the reduction of the nucleon effective mass which overcomes the intrinsic enhancement of the *G*-matrix elements. We provided quadratic parametrizations of the density dependence of the cross sections at energies above 200 MeV, with energy dependent coefficients. These features may be probed by calculating collective observables such as the balance energy or the radial flow in different ranges of density. The results at lower energies are strongly influenced by our choice of idealized conditions, namely infinite system (single Fermi sphere) at zero temperature, with the modification of single-nucleon spectra due to pairing gaps neglected. We will focus on these issues in a future publication.

A more general approach would take into account the relative motion of two pieces of nuclear matter, that is, in

principle, more appropriate to simulate NN scattering in heavy ion collisions. But, the calculations performed so far suffer strong simplifications. In one case [7] (BHF with Reid soft-core potential) the mean field used for the two colliding nuclear matters is assumed to be the same as the one for a single nuclear matter of the same density in equilibrium, thus missing the dynamical effects included in a real self-consistent calculation. (In fact, global effective masses reported in Ref. [7] are very similar to ours.) The DBHF calculations of Ref. [13] suffer from the same shortcoming. Here an additional averaging on the momentum of the incoming nucleon is performed in order to define a cross section that depends only on the global variables characterizing the configuration in momentum space. This approach presents ambiguities in the case of overlapping Fermi spheres, which is unfortunately the physically most relevant. In view of our findings that the main source of the suppression of in-medium cross sections is the reduction of the density of states due to the effective nucleon mass, a truly self-consistent calculation of cross sections in this approach seems very valuable. This would imply the dependence of in-medium cross sections (and single-particle potentials) on even more variables.

Some important aspects of the in-medium cross sections have been left aside in this paper. The first one is to investigate where the effects of the enhancement due to the pairing singularity might be relevant. A good candidate could be the expansion phase of central events in heavy ion collisions where the system rapidly cools down below the critical temperature, or a low-energy proton-ion reaction where the collisions are supposed to occur in cold nuclear matter. A second aspect is the extension of the calculations to finite temperature [8,10], as well as the inclusion of ground state correlations in the effective mass [12,24]. Finally, recent experiments performed to determine the balance energy for very asymmetric systems demand for an extension of the present calculations to isospin-asymmetric nuclear matter [26]. From this investigation important information can be extracted on the separate effects of σ_{nn} and σ_{np}, the latter being mainly affected by the tensor component of the nuclear force.

ACKNOWLEDGMENTS

We acknowledge useful discussions with P. Danielewicz, A. Sedrakian, and H. Wolter.

[1] P. Danielewicz, in *Proceedings of the 1st International Conference on Critical Phenomena and Collective Observables, CRIS96*, Acicastello, 1996, edited by A. Insolia *et al.* (World Scientific, Singapore, 1996).
[2] G. D. Westfall *et al.*, Phys. Rev. Lett. **71**, 1986 (1993).
[3] S. Soff, S. A. Bass, C. Hartnack, H. Stöcker, and W. Greiner, Phys. Rev. C **51**, 3320 (1995).
[4] T. Alm, G. Röpke, W. Bauer, F. Daffin, and M. Schmidt, Nucl. Phys. **A587**, 815 (1995).
[5] A. Insolia, U. Lombardo, N. G. Sandulescu, and A. Bonasera, Phys. Lett. B **334**, 12 (1994).
[6] V. de la Mota, F. Sebille, M. Farine, B. Remaud, and P. Schuck, Phys. Rev. C **46**, 677 (1992).
[7] T. Izumoto, S. Krewald, and A. Faessler, Nucl. Phys. **A341**, 319 (1980); M. Trefz, A. Faessler, and W. H. Dickhoff, *ibid.* **A443**, 499 (1985); A. Bohnet, N. Ohtsuka, J. Aichelin, R. Linden, and A. Faessler, *ibid.* **A494**, 349 (1989); J. Jänicke, J. Aichelin, N. Ohtsuka, R. Linden, and A. Faessler, *ibid.* **A536**, 201 (1992); D. T. Khoa *et al.*, *ibid.* **A548**, 102 (1992); E. Lehmann, A. Faessler, J. Zipprich, R. K. Puri, and S. W. Huang, Z. Phys. A **355**, 55 (1996).
[8] J. Cugnon, A. Lejeune, and P. Grange, Phys. Rev. C **35**, R861 (1987); A. Lejeune, P. Grange, M. Martzolff, and J. Cugnon, Nucl. Phys. **A453**, 189 (1986).
[9] B. ter Haar and R. Malfliet, Phys. Rev. C **36**, 1611 (1987).
[10] M. Schmidt, G. Röpke, and H. Schulz, Ann. Phys. (N.Y.) **202**, 57 (1990); A. Sedrakian, D. Blaschke, G. Röpke, and H. Schulz, Phys. Lett. B **338**, 111 (1994); T. Alm, G. Röpke, and M. Schmidt, Phys. Rev. C **50**, 31 (1994); A. Sedrakian, G. Röpke, and T. Alm, Nucl. Phys. **A594**, 355 (1995).
[11] G. Q. Li and R. Machleidt, Phys. Rev. C **48**, 1702 (1993); **49**, 566 (1994).
[12] G. Giansiracusa, U. Lombardo, and N. Sandulescu, Phys. Rev. C **53**, R1478 (1996).
[13] C. Fuchs, L. Sehn, and H. H. Wolter, Nucl. Phys. **A601**, 505 (1996); L. Sehn and H. H. Wolter, *ibid.* **A601**, 473 (1996).
[14] M. Lacombe *et al.*, Phys. Rev. C **21**, 861 (1980).
[15] R. B. Wiringa, R. A. Smith, and T. L. Ainsworth, Phys. Rev. C **29**, 1207 (1984).
[16] J. Heidenbauer and W. Plessas, Phys. Rev. C **30**, 1822 (1984); **32**, 1424 (1985).
[17] K. A. Brueckner and J. L. Gammel, Phys. Rev. **109**, 1023 (1958).
[18] J.-P. Jeukenne, A. Lejeune, and C. Mahaux, Phys. Rep. **25C**, 83 (1976).
[19] H. P. Stapp, Phys. Rev. **103**, 425 (1956); **105**, 302 (1957); Ta-You Wu and T. Ohmura, *Quantum Theory of Scattering* (Prentice-Hall, Englewood Cliffs, NJ, 1962).
[20] G. R. Satchler, *Direct Nuclear Reactions* (Clarendon Press, Oxford, 1983).
[21] V. J. Emery, Nucl. Phys. **12**, 69 (1959); R. F. Bishop, M. R. Strayer, and J. M. Irvine, Phys. Rev. A **10**, 2423 (1974).
[22] M. F. Jiang and T. T. S. Kuo, Nucl. Phys. **A481**, 294 (1988).
[23] B. E. Vonderfecht, C. C. Gearhart, W. H. Dickhoff, A. Polls, and A. Ramos, Phys. Lett. B **253**, 1 (1991).
[24] M. Baldo, I. Bombaci, G. Giansiracusa, U. Lombardo, C. Mahaux, and R. Sartor, Phys. Rev. C **41**, 1748 (1990); Nucl. Phys. **A545**, 741 (1992); H. S. Köhler and R. Malfliet, Phys. Rev. C **48**, 1034 (1993).
[25] C. Lechanoine-LeLuc and F. Lehar, Rev. Mod. Phys. **65**, 47 (1993).
[26] I. Bombaci and U. Lombardo, Phys. Rev. C **44**, 1892 (1991).